

## Development of SMH Actuator System Using Hydrogen-Absorbing Alloy

Tae-Kyu Kwon\*, Won-Suk Jeon\*\*, Du-Yeol Pang\*\*, Kwang-Hun Choi\*\*, Nam-Gyun Kim\*,  
and Seong-Cheol Lee\*\*

\* Division of Bionics and Bioinformatics, Chonbuk National University, Jeonju, Korea  
(Tel : +82-63-270-2247, Email: kwon10, ngkim@chonbuk.ac.kr)

\*\* Dept. of Mechanical Engineering, Chonbuk National University, Jeonju, Korea  
(Tel : +82-63-270-2320, Email : jswsss@lycos.co.kr, fishhh, apollo\_choi@hotmail.com, meconlee@chonbuk.ac.kr)

**Abstract:** This paper presents the temperature-pressure characteristics of a new SMH actuator using a Peltier module. The SMH actuator is characterized by its small size, low weight, noiseless operation, and compliance similar to that of the human body. The simple SMH actuator, consisting of the plated hydrogen-absorbing alloys as a power source, Peltier elements as a heat source, and a cylinder with metal bellows as a functioning part has been developed. To improve the thermal conductivity of the hydrogen-absorbing alloy, an assembly of copper pipes has been used. It is well known that hydrogen-absorbing alloys can reversibly absorb and desorb a large amount of hydrogen, more than about 1000 times of their own volume. The hydrogen equilibrium pressure increases when hydrogen is desorbed by heating of the hydrogen-absorbing alloys, whereas by cooling the alloys, the hydrogen equilibrium pressure decreases and hydrogen is absorbed. The new special metal hydride (SMH) actuator uses the reversible reaction between the heat energy and mechanical energy of a hydrogen absorbing alloys. The desirable characteristics of SMH actuator, which makes it suitable for the uses in medical and rehabilitation applications, have been also studied. For this purpose, the characteristics of the new SMH actuator for different temperature, pressure, and external load were explored.

**Keywords:** Special metal hydride(SMH) actuator, Hydrogen-absorbing alloys, Rehabilitation equipment, Peltier element

### 1. INTRODUCTION

The hydrogen-absorbing alloys, Metal Hydrides(MH) alloys, have been discovered by the researchers in Phillips Poland and the Brookhaven national laboratory in USA in 1970s. Today, many researchers are exploring various kinds of constructions of hydrogen-absorbing alloys and trying to improve the characteristics of them. The applicable areas of hydrogen-absorbing alloys are diverse like containment of hydrogen, heat pump, compressor, and Ni-MH rechargeable battery. Since the containment of hydrogen in MH alloy has the effect of purification, the possible application of MH actuator is also very likely in the area of electronics and semi-conductor industry which uses hydrogen of high purity. Therefore, many researches are also going on in those industries as well. Recently, preliminary studies on the application of MH alloys in actuation device are being carried out.

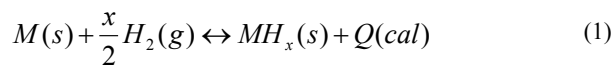
There are other types of storage methods of hydrogen. Hydrogen can be stored in a high-pressure tank in gas state or can also be cryogenically stored as liquid hydrogen. Compared with these methods, the storage method utilizing metal hydrides offers the advantages in that it is much safer and that the storage capacity per unit volume is larger with Metal Hydride Alloys [2~4].

There have been many researches on metal hydride alloys in South Korea. However, most of the researches were limited to either the development of Ni-MH rechargeable battery or the design and development of hydrogen storage unit, and some of the items from these researches are near the point of commercialization. Here, we have studied the development and the application of a new actuation system utilizing MH alloys and examined the characteristics of the newly developed system. The new Special Metal Hydride (SMH) actuator developed from the present study is a new type of

actuator, which was constructed by inserting powdered Metal Hydride into copper pipes.

### 2. THEORY ON HYDROGEN ABSORBING ALLOYS

MH alloys can attract and store hydrogen atoms through chemical hydriding reaction at the surface. By cooling the MH alloys or increasing pressure, the alloys absorb hydrogen generating heat, whereas by heating the MH alloys or decreasing pressure, the alloys desorb hydrogen absorbing heat. As explained, MH alloys can reversely react with hydrogen. The characteristics of this reaction can be described as the following reaction.



Here,  $Q(cal)$  is heat of reaction. As can be seen in the reaction equation, by utilizing the reaction of absorption and desorption of hydrogen, it is possible to convert thermal energy, in the form of heating or cooling, into mechanical energy in the form of the change in the pressure of hydrogen gas.

Hydrogen absorbing alloys can reversely absorb and desorb hydrogen at certain temperature and pressure. These characteristics of hydrogen can be exhibited in a hydrogen Pressure-Composition-Temperature (P-C-T) diagram which shows the amount of equilibrium hydrogen in the alloys.

### 3. DEVELOPMENT OF HYDROGEN ABSORBING ALLOYS

#### 3.1 Construction of hydrogen absorbing alloys

The known hydrogen absorbing MH alloys up to date

consist of pure metals such as Mg, Ti, or Zr or intermetallic compounds of the metals such as Fe and Ti. Generally speaking, the pure metal MH alloys such as  $MgH_2$  have bigger capacity for hydrogen but have shortcomings of poor reaction time and low equilibrium pressure, whereas the intermetallic compounds not only have very high reaction speed for absorption and desorption of hydrogen but also has appropriate capacity and equilibrium pressure for hydrogen as well as superior chemical stability. These ideal characteristics of MH alloys of intermetallic compounds have been attracting many researchers, and in the result, among many promising MH alloys,  $LaNi_5$  and  $Mg_2Ni$  MH alloys have been suggested by number of researchers [4-5]. Among the two,  $Mg_2Ni$  alloys have outstanding capacity limit for hydrogen, but it can only be used in high temperature applications because of its high reaction temperature. In the other hand,  $LaNi_5$  alloys has good characteristics as hydrogen absorbing alloys but the cost of La and the cost of the manufacturing the alloys is expensive. Furthermore, the repeated cycles of absorption and desorption degrades the desired characteristics of the alloys. Therefore, the researches on replacing La with inexpensive rare-earth Mm (misch metal) and replacing Ni with small amount of Al, Fe, or Mn are going on.

Vacuum Arc Furnace (VAF) was used in melting MH alloys in the present study. The purities of the substances used in the MH alloys were very high: Zr above 99.7%; Ti, 99.99%; Cr, 99.7%; Fe, 99.7%. The composition ratios of the alloys were as follows: Zr, 0.95; Ti, 0.051; Fe, 1.4; and Cr, 0.6. Before melting the compounds, the mass of each compound was accurately measured and prepared using electronic scale to make up the alloy sample with the total mass of 14.85g. Next, the compounds were put into the mold of a Vacuum Arc Furnace, and were arc melted for 30 minutes in vacuum condition at 1800°C of temperature. For the homogeneity inside of the alloy, the alloy sample were turned over and remelted for five times.

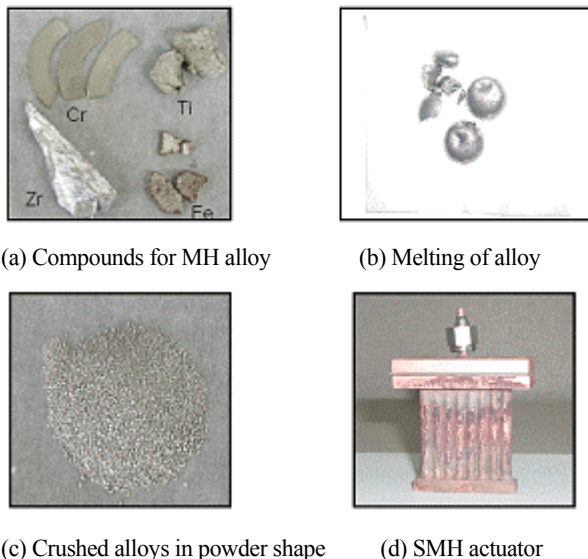


Fig. 1 The process of making SMH actuator

Figure 1 shows the manufacturing process of SMH actuator. The detailed process is as follows.

1. The compounds are precisely measured and prepared so that the mass of the compounds become as follows: Zr 6.49g, Ti 0.17g, Fe 2.33g, and Cr 5.86g.

2. The alloy sample is made in the vacuum arc furnace by arc melting.
3. The alloy is crushed into powder shape using a crusher, and the crushed alloys are filtered with 500 $\mu m$  mesh.
4. The filtered powder shape alloys are inserted into copper pipe type SMH actuator. Glass wool is used to seal the end of the pipe to prevent the powder shape alloys from entering the tube while operation.

### 3.2 Activation Process

The SMH actuator can be used after going through a required activation process. The activation process indicates the process of removal of oxides and desorption of hydrogen by heating the alloys. The alloys used in this experiment have the characteristic of being activated easily without special heat treatment as shown in Fig 1. of P-C-T diagram.

Figure 2 shows an apparatus for the activation process for the SMH actuator. The activation process is as follows. First, the system is assembled preventing gas leakage. Next, hydrogen gas with the pressure of 30atm is applied through a tube. In the meantime, the leakage of gas is checked for extended period of time. The next step is leaving a vacuum inside of the system for 40 minutes with a vacuum pump. This is followed by closing the valve connected to the vacuum pump. The next is applying constant pressure of hydrogen gas (40atm) into the system so that hydrogen can be absorbed to the alloys. The final step in the activation process is making the SMH actuator to absorb and desorb hydrogen by controlling hydrogen pressure. The absorption and desorption process is repeated four times until the speed and the amount of absorption and desorption become constant.

### 3. OPERATION PRINCIPLE OF SMH ACTUATOR

The general characteristics of SMH actuators are soft response to loads, compact size of the actuation system that includes drive system, and low noise. These characteristics make the SMH actuator to be an excellent candidate for the uses in rehabilitation devices which operate with physical contact to humans.

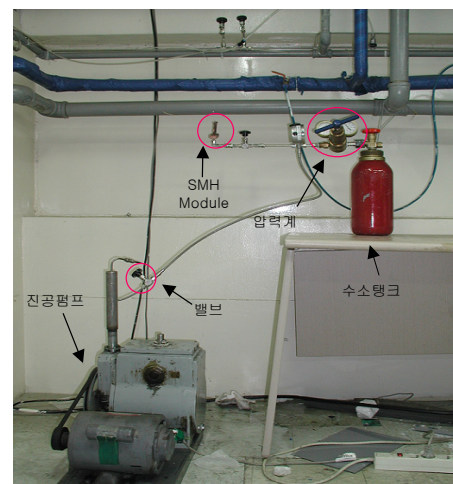


Fig. 2 The apparatus for the activation process of SMH actuator

Figure 3 shows the process of the transformation of energy in the hydrogen absorbing alloys. This explains the operation of the SMH actuator from the principle of the conversion of chemical reaction energy to mechanical energy and again to thermal energy.

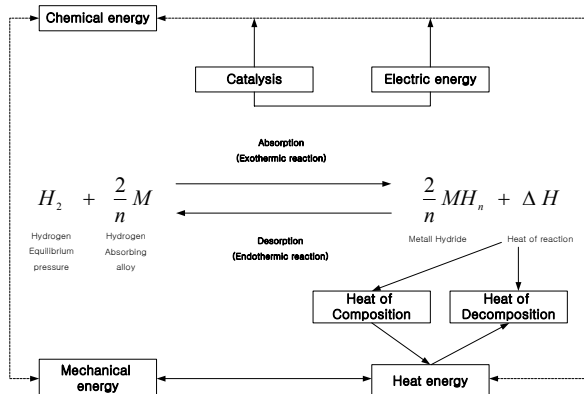


Fig. 3 Transformation of energy in hydrogen absorbing alloys

Therefore, it is possible to build an actuator based on this reversibility of hydrogen absorption reaction in the hydrogen absorbing alloys. The basic principle of operation is converting pressure gain, produced by heating or cooling the alloys inside a sealed container with a heater or cooler, into mechanical force in a mechanism. In heating and cooling the hydrogen alloys, we used the Peltier element which is made by arranging p-type semiconductor and n-type semiconductor in turn. The alloy can be heated or cooled by changing the direction of the electric current to the Peltier element. By utilizing this characteristic of the element, we can control the absorption and desorption of hydrogen. So, we have constructed a driving module for the SMH actuator by attaching hydrogen absorbing alloys inside of the sealed container and Peltier element outside of the sealed container.

Figure 4 shows a schematic diagram of the SMH actuator. The SMH actuator consists of an operational part and a functional part. The operational part consist of an electric power source, which supply electricity to the Peltier elements and Cooling fan, and a control box, which senses pressure and temperature and control the Peltier element. The functional part transfers the hydrogen pressure to a cylinder for actuation.

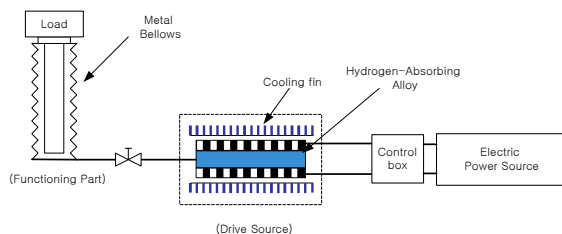


Fig. 4 The operation of the SMH actuator

The operational process of the SMH actuator is as follows. First, the electric current is allowed from the electric power source to the Peltier element. The current to the Peltier element is restricted by control box in such a way that the temperature of the element is between 35°C and 75°C, of which temperatures were determined from previous

experiments. The electric current in the Peltier element raises the temperature and causes the hydrogen absorbing alloys to desorb hydrogen. This results in the increase of the hydrogen pressure, which raises the piston. On the contrary, the cooling of alloys results in the decrease of hydrogen pressure from absorption of hydrogen to the alloys, which causes the contraction of the cylinder.

#### 4. EXPERIMENTAL APPARATUS AND METHODS

In the present study, we have selected the mass ratio of the compounds to be Zr<sub>0.95</sub>, Ti<sub>0.05</sub>, Fe<sub>1.4</sub>, and Cr<sub>0.6</sub> to make an alloy which has relatively quick reaction speed and high pressure output at normal temperature. Utilizing this alloy, we have built an MH module and actuator. Here, we have also studied temperature pressure characteristics of the actuator.

The container for the hydrogen alloys in SMH actuator was constructed by welding eight copper pipes together. Copper is known to have an excellent heat conduction rate. The embossing parts of the copper pipe went through heat treatments. Silver welding was used to maintain excellent heat conduction rate. The advantage of this actuator compared to the previous MH actuators is the use of copper pipe, which has excellent conduction ratio, and the enabling of the thermal control by the control of electric current using the Peltier element.

Figure 5 shows the developed SMH actuator, which consist of eight copper pipes with the diameter of 4.75mm, the height of 73mm, and the width of 42mm. The connecting part between the copper pipe assembly and the valve was sealed by 12 bolts with the diameter of 3.8mm to prevent the leakage of hydrogen.



Fig. 5 The appearance of the copper pipe assembly

Table 1 The specifications of the SMH actuator

Type	Size (mm)	Metal hydride		
		Mass(g)	Mesh(μm)	Composition
Cu pipe	64×41×7t	14.85	500	Zr <sub>0.95</sub> , Ti <sub>0.05</sub> , Fe <sub>1.4</sub> , Cr <sub>0.6</sub>

Table 1 shows the size of the SMH actuator and the composition of the alloys. The combined weight of the alloys in SMH actuator is 14.85g and 500μm of mesh was used in

filtering the powder shape of the alloy. The experimental apparatus for the performance evaluation of the SMH actuator is shown in Fig. 6. For the performance evaluation, the Peltier elements were attached to the front and the rear side of the copper pipe assembly and the heat sink and cooling fan were attached to the other sides of the Peltier elements as shown in the figure. The automatic control of the cooling fan was also enabled.

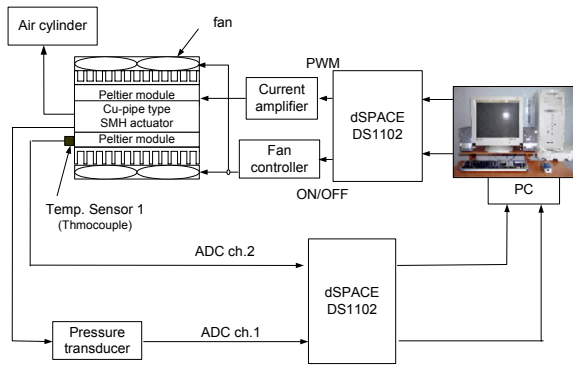


Fig. 6 The block diagram of the experimental apparatus

Table 2 shows the specifications of the pressure transducer (PMP1400, Hirschman), the Peltier module (VSM-1.4-161-6.0, Vortex), and the cylinder (CM2F40-100, SMC) used in the experiment. The temperature was about 30°C during the experiment.

Table 2 Specifications of the pressure transducer, the cylinder, and the Peltier module

Pressure Transducer		Cylinder		Peltier module	
pressure range	100m Bar ~ 600 Bar	size	φ 40	size	40×40×4.12(mm)
supply voltage	9 ~ 28V DC	stroke	100mm	maximum voltage	67.1 V
Output	0 ~ 5V (3 wires)	maximum pressure	0.18MPa	maximum current	6.0 A
Accuracy	± 0.15% Fs	piston speed	50~750 mm/s	maximum temperature	70.4°C
operating temperature	-20 ~ 80°C	cylinder type	single-acting cylinder		

To evaluate the performance of the Peltier element, we used Matlab5.3 Simulink (Mathworks Inc.) and dSPACE 1103 control board (dSPACE Inc.) and controlled the current in the Peltier module. We used self-made current amplifier, which consisted of transistors, Op-Amp, and ceramic resistors and can control the current based on the feedback signal to the Op-Amp. The control of the temperature of the Peltier element was done in such a way that positive current is allowed until the upper temperature is reached; if the temperature reaches the upper limit, the current is switched to negative current. When the current is switched to negative, the cooling fans are turned on to help cooling of the module until the bottom limit of temperature is reached.

### 5. RESULTS AND OBSERVATIONS

The relationship between the electric current input and the temperature in the SMH actuator is shown in Fig. 7. The change in the SMH actuator was observed changing the electric current to the Peltier element from 0.2A to 2A with the increment of 0.2A. In the figure, x-axis represents actuation time(sec), and y-axis represents the temperature (°C) in the actuator.

The convergences of the temperatures to 30°C were observed for the currents between 0.2A and 0.6A. This seems to be due to the fact that generation of heat with small electric current in the Peltier element won't overcome the loss of heat at the side adjacent to heat sink and the temperature converges to 30°C, which is the temperature of the room. We can observe constant increase of heat with the currents between 0.8A and 2A.

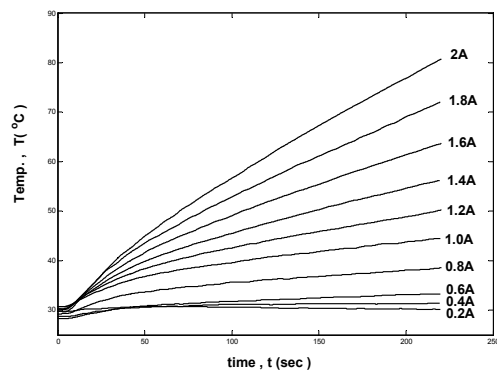


Fig.7 The relationship between electric current input and temperature in the SMH actuator

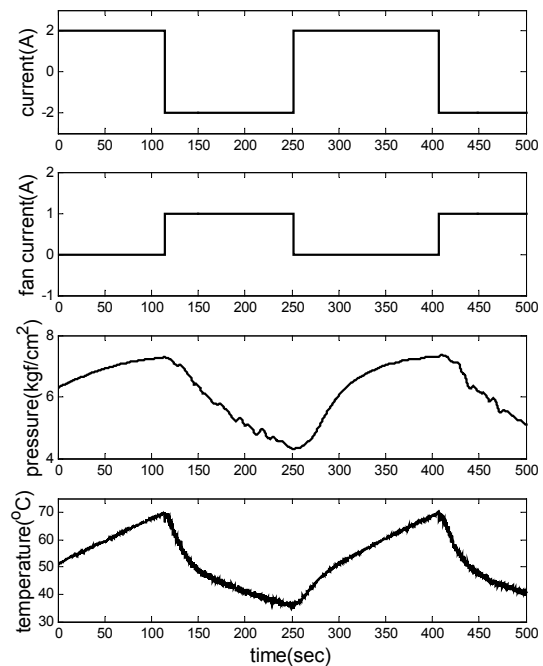


Fig. 8 The current, pressure, temperature vs. time diagram in SMH module for the temperature between 35°C and



Figure 8 shows the temporal changes in the current in the Peltier module, the current in the fan, the pressure, and the temperature of SMH actuator when the weight load of 30kg is applied to the cylinder, the upper and bottom limit of temperatures were set to be 75°C and 35°C respectively, and the amplitude of the pulse shaped current input was 2A. In the figure, we can observe positive current results in the heating of element, the negative current results in the cooling of the element, and the operation of cooling fan which increases efficiency of cooling. We can also observe some hysteresis is occurring.

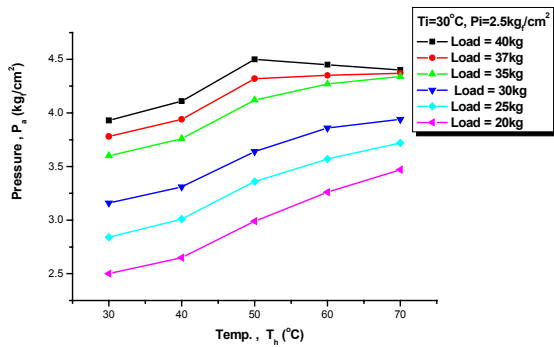


Fig. 9 The relationship between the upper limit of temperature and the pressure of SMH actuator

The relationship between the temperature and the pressure in the SMH actuator for different loads to the cylinder is shown in Fig. 9. The x-axis represents the upper limit of the temperature and y-axis represents the pressure in the cylinder. We can observe that the pressures increased in similar rate (about 0.35kgf/cm<sup>2</sup> per 40°C of temperature increment) when the load to the cylinder was same as or below 35kg. However, we can observe the pattern of the progress of the pressure increment changes dramatically when the load is over 35kg and the temperature is over 50°C. We can even observe the drop of the pressure in the cylinder when the temperature is over 50°C for the load of 40kg.

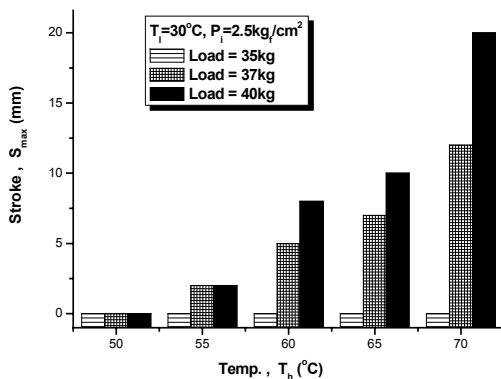


Fig. 10 The relationship between the maximum cylinder stroke and the upper limit of the temperature

Figure 10 shows the maximum strokes of the cylinder for

different loads when the temperature changes from various upper limits to the bottom limit. When the upper limit of the temperature is 50°C, we can observe that the maximum stroke is maintained constant. We can observe the maximum stroke of up to 12mm when the temperature upper limit is 60°C or 70°C and the load is 37kg. The maximum stroke of up to 20mm is observed when the load is 40kg. We found that the drop of pressure occurs due to the increase in the volume of the cylinder when the cylinder expands. When the initial pressure is 2.5kgf/cm<sup>2</sup>, the appropriate operation condition of the cylinder is as follows: the load is over 47kg; the upper limit of temperature is over 50°C; and the bottom limit of temperature is 30°C.

The maximum stroke of the cylinder for different initial loads and for different temperature limits are shown in Fig. 11. We can see from Fig. 11 that the maximum stroke increases as the load increases and as the temperature increases when the upper limit of the temperature is between 50°C and 60°C. In the contrary, we can observe that the maximum stroke decreases as the load increases when the upper limit of the temperature is between 37°C and 40°C. The reason for this seems to be that when the initial pressure is 1kgf/cm<sup>2</sup> and the load to the cylinder is big (30kg or 40kg), the absorption of hydrogen by hydrogen absorbing alloys is affected by the added load to the cylinder and result in bigger displacement of piston. In the other hand, when the load is small (20kg or 15kg), the absorption of hydrogen is not affected by the added load to the cylinder. Therefore, when the initial pressure is 1kgf/cm<sup>2</sup>, for the loads heavier than 30kg, it is best to set the upper limit temperature higher than 50°C, and for the loads lighter than 30kg, it is best to set the upper limit temperature lower than 40°C. Figure 12 shows the picture of the actual displacement of the SMH actuator against 40kg load.

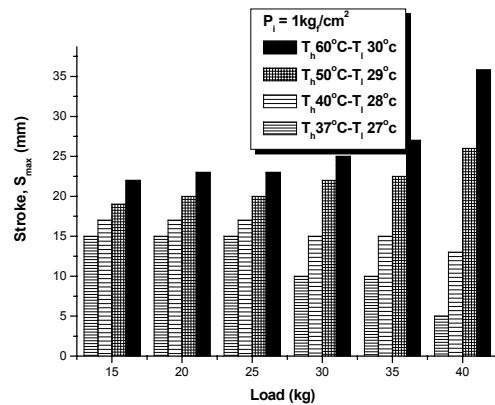


Fig. 11 The relationship between the maximum cylinder stroke and the load (initial pressure of the cylinder is 1kgf/cm<sup>2</sup>)

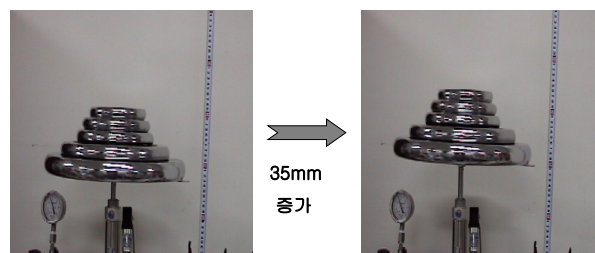


Fig.12 The lifting of 40kg weight load with the SMH actuator.

**6. CONCLUSIONS**

In this study, we have developed a new SMH actuator system and observed its pressure-temperature characteristics. The followings are the findings from the experiment.

1. We observed the increase of hydrogen pressure in the new SMH actuator when electric current is introduced in the Peltier elements, and detected the effective change of hydrogen pressure that closely followed the temperature change of the SMH actuator.
2. We confirmed the possibility of the actuation control method of maintaining upper and bottom limit of the temperature for SMH actuator module. The dependency of the period of actuation depends on the electric input current was confirmed as well.
3. The trends in the temperature changes in the SMH actuator according to the change in the input current were found. Also, the input currents and the periods of actuation were found according to the set temperature limits.
4. We were also able to confirm that an SMH actuator can produce a large force output considering its small size. Moreover, the advantages of the SMH actuator in its small noise characteristic and portable nature were also observed.

The future researches will be on reducing the period of thermal control and making the SMH actuator to be more efficient and more portable. This will be followed by the researches on producing the SMH actuator with desirable characteristics more suitable for the silver and rehabilitation devices. Eventually, this will open the door for the SMH actuator to broad application to silver devices as well as rehabilitation devices such as movement assistant devices.

**ACKNOWLEDGMENTS**

This research was supported by the Korean Ministry of Commerce, Industry and Energy through a grant on the development of the core technology for medical devices for elderly.

**REFERENCES**

[1] S. Shimizu, et al, "Evaluation of a New Force Display using Metal Hydride Alloys," *Journal of Robotics and Mechatronics*, Vol. 9, No. 1, 1997.

[2] Y. Wakisaka, M. Muro, T. Kabutomori, H. Takeda, S. Shimizu, S. Ino, and T. Ifukube, "Application of Hydrogen Absorbing Alloys to Medical and Rehabilitation Equipment," *IEEE Transaction on Rehabilitation Engineering*, Vol. 5, No. 2, pp.148-157, 1997.

[3] K. Kurosaki, T. Maruyama, K. Takahashi, H. Muta, M. Uno, and S. Yamanakaet, "Desingn and Development of MH actuator system," *Sensors and Actuators A*, Vol. 113, pp. 118-123, 2004.

[4] H. Fujii, and S. Orimo, "Hydrogen storage properties in nano-structured magnesium and carbon-related materials," *Physica B: Condensed Matter*, Vol. 328, pp. 77-80, 2003.

[5] P. Termsuksawad, S. Niyomsoan, R.B. Goldfarb, V.I.

Kaydanov, D.L. Olson, B. Mishra, and Z. Gavrac, "Measurement of hydrogen in alloys by magnetic and electronic techniques," *Journal of Alloys and Compounds*, Vol. 373, pp. 86 -95, 2004.

[6] G. Min and D. M. Rowe, "Improved model for calculating the coefficient of performance of a Peltier module," *Energy Conversion & Management*, Vol. 41, pp. 163-171, 2000.

[7] D. Stefan, S. Amine, G. Stephane, and C. Wilfrid, "Laser Seebeck Effect Imaging(SEI) and Peltier Effect Imaging(PEL) Complementary investigation methods," *Microelectronics Reliability*, Vol. 43, pp. 1609-1613, 2003.

[8] C. Reiyu, H. Guanming and D. Stefan, "Thermoelectric cooler application in electronic cooling," *Applied Thermal Engineering*, Vol.24, pp. 2207-2217, 2004.

[9] M. Farid, N. Nobuyuki, S. Hidenori, M. Akihiko, and T. Kazuo, "Preparation and characterization of carbonaceous material-based hydrogen absorbing composites," *Journal of Alloys and Compounds*, Vol. 372, pp. 243-250, 2004.

[10] Y. Osumi, H. Suznki, A. Kato, K. Oguro, T. Suioka and T. Fujita, "Hydrogen storage properties of Ti1+x Cr2-y Mny alloys" *Journal of the Less Common Metals*, Vol. 89, pp. 257-262, 1983.

[11] R. C. Baker and B. Charlie, "Nonlinear unstable systems," *International Journal of Control*, Vol. 23, No. 4, pp. 123-145, 1989.